

# Investigations of surface topography of titanium alloy manufactured with the use of 3D print

**P Grobelny<sup>1</sup>, S Legutko<sup>1</sup>, W Habrat<sup>2</sup> and L Furmanski<sup>1</sup>**

<sup>1</sup>Faculty of Mechanical Engineering and Management, Poznan University of Technology, 3 Piotrowo street, 60-965 Poznan, Poland

<sup>2</sup>Department of Manufacturing Techniques and Automation, Rzeszow University of Technology, 2 W. Pola street, 35-959 Rzeszow, Poland

E-mail: stanislaw.legutko@put.poznan.pl

**Abstract:** The paper presents the possibilities of 3D printing of chosen titanium alloy for manufacturing ready made parts. Results of examination of the surface topography of material manufactured using the AM 250 device by RENISHAW for laser sintering using the SLM method have been presented. 3D printing of metal parts has the potential to revolutionize the market of manufacturing and supplying parts. It makes it possible to dissipate manufacturing and to produce parts on request at lower cost and less energy consumption. The chosen parameters of the surface topography of titanium alloy under investigations directly after printing can differ depending on the distance from the base plate. Surface roughness parameters, isotropy and Abbott-Firestone curve after machining were also identified.

## 1. Introduction

The technique of additive manufacturing with the use of metal is more and more popular and it may become one of the main technologies and an integral part of the set of methods and tools of each engineer and designer. Due to the application of additive techniques, it is possible to obtain geometrically complex shapes, time of manufacturing is shortened, the number of elements in a subassembly is reduced and, consequently prevalence over competitors is obtained despite the higher cost of manufacturing the elements. What is more, the technology of laser sintering of metal powders, enables the development of advanced and light constructions which combine high strength with mass reduction by as much as 60%. Even very complicated elements made of high strength material can be easily made with the use of additive techniques where the use of the traditional manufacturing processes is impossible or very expensive. The growing development of additive techniques of metal materials brings the necessity to learn the surface topography of the products made of those materials [1], [2]. This concerns both just made surfaces and ones subjected to machining [3], [4].

The purpose of the investigation was to identify and compare selected surface topography parameters after the process of turning the titanium alloy, Ti6Al4V obtained by the additive techniques to the parameters of the same material made by the metallurgical technique.

## 2. Characterization of methods and material used for testing

The SLM method (Selective Laser Melting) makes it possible to manufacture complex geometry parts of metallic powder. The elements made in this way are subjected to machining on the surfaces to be matching the surfaces of other elements. As a rule, the arm distributing the powder, which has a blade



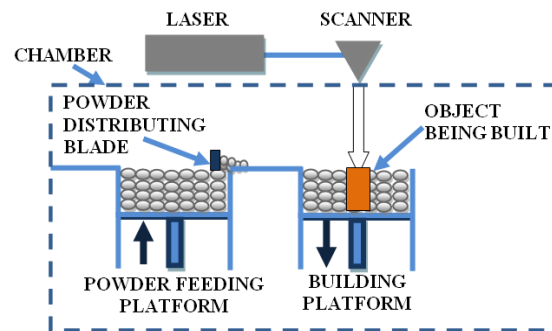


**Figure 1.** General diagram of the Selective Laser Melting method.

at the end, cuts the melting unevennesses of the previous layer. The principle of the SLM method is shown in Figure 1.

An important issue in the SLM technology is the necessity to generate durable supporting structures. This is due to the significant temperature differences between the working chamber and the liquid metal. Therefore must be removed, after a part is made, it has to be cut off the start plate and the supports. Examples of supports for the parts under investigation can be seen in Figure 2. The presented part has been cut off the start plate.

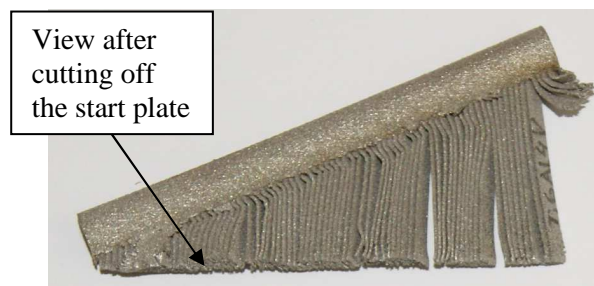


**Figure 2.** Application of supports when printing the part under investigation.

The supports can have various shape and it is determined during the outprint designing. The sample described above has been made at the angle of 30°. The time of execution of a given sample depends, among others, on the number of parts made in one printing. For example, for a sample made of titanium alloy, Ti6Al4V, simulation of the number of printed elements in relation to the time of printing those elements has been shown in Figure 3. Such simulation is made possible by the software for the devices of Renishaw company.

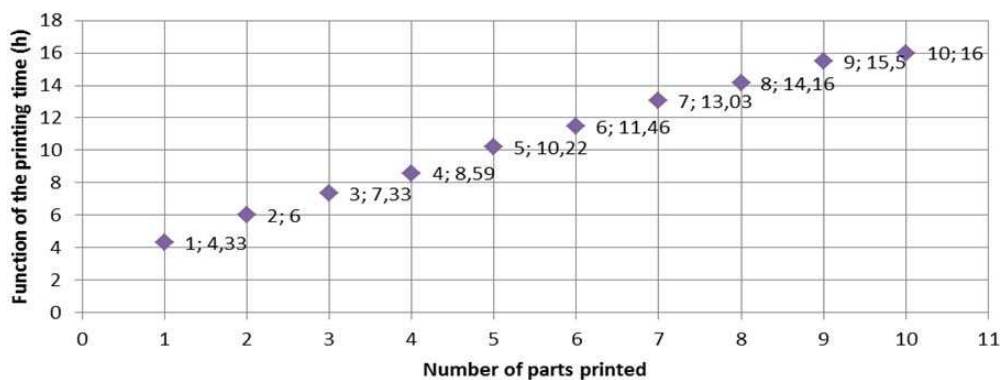


**Figure 3.** Number of parts printed as a function of the printing time.

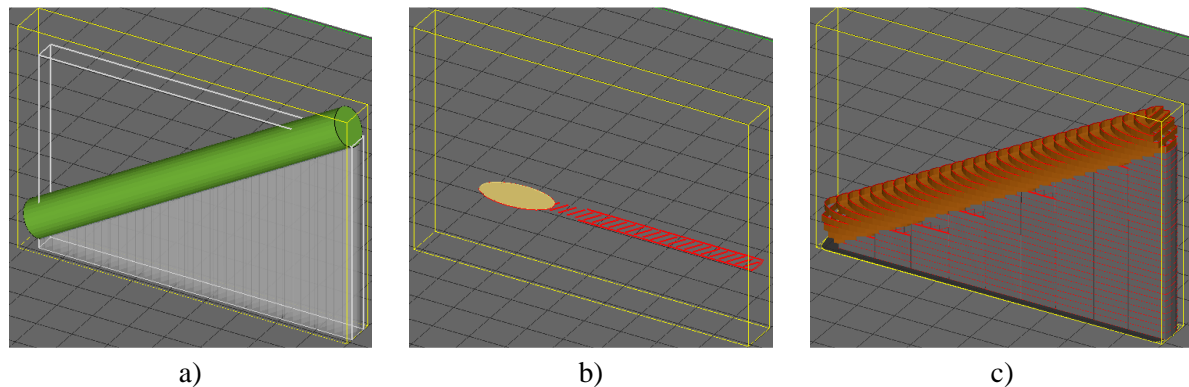


**Figure 4.** Simulation of a sample output (the author's own elaboration): a) virtual model, b) the first layer of the virtual laminar model, c) Approximate shape of the real object – visible step effect.

For a selected sample, one can also check how the individual layers in the device will be built and the locations of the supports (Figure 4). The software divides the network geometry into layers of predetermined thickness creating a laminar model. Next, for each layer, working paths are generated controlling the device. In the methods used in sample making, those are mirrors directing the laser beam. Next the manufacturing process takes place till the ready-made output is obtained.

In the present investigation, titanium alloy, Ti6Al4V, has been used; the alloy has chemical composition in accordance with the European standard 3.7164. Till not very long ago, the material has been considered as a strategic one, applied in the aircraft industry, shipbuilding and aerospace industry as well as for military needs [5 -8]. The alloy is perfectly suitable for engineering applications which require high strength, e.g. in the automotive branch and in medicine [9-11]. Due to the additive technology used in manufacturing elements, those elements can have various surface roughness. Two groups of samples have been subjected to experimental tests. The group designated C1 has been made in the form of a shaft with the diameter of 10 mm and the length of 100 mm on the AM 250 device for laser sintering by the SLM method made by RENISHAW company. Sample group C1'' has been made by casting and hot drawing.

### 3. Methodology of investigation

Surface topography has been examined both for the samples just manufactured and after the process of finish machining. The following technological parameters of machining have been applied:

- cutting speed,  $v_c = 60\text{m/min}$
- feed,  $f = 0.1; 0.15; 0.2\text{ mm/rev}$
- depth,  $a_p = 0.5\text{ mm}$

The printed samples have been subjected to machining on the MAZAK QTS 250M. The process has been executed by PIWEK Centre of Numerical Processing Krzysztof Piwek in Rososzyc. With the participation of the production engineer of MMC Hardmetal Poland Ltd, adequate process parameters and tools have been selected for the materials of which the samples had been made. The titanium alloy, Ti6Al4V, has been machined with the use of:

- lathe tool DWLNR2525M08,
- lathe plate WNMG080408-MS MT9015

The surface topography parameters have been determined on 8 elementary areas and the obtained data have been averaged. For both sample groups, C1 and C1'', areas A (top), B (middle), C (bottom) have been established which have been subjected to machining under production conditions (Figure 5).

Surface topography parameters have been measured with the use of a focal differentiation microscope and a version of computer software, MountainsMap Premium 7.4.

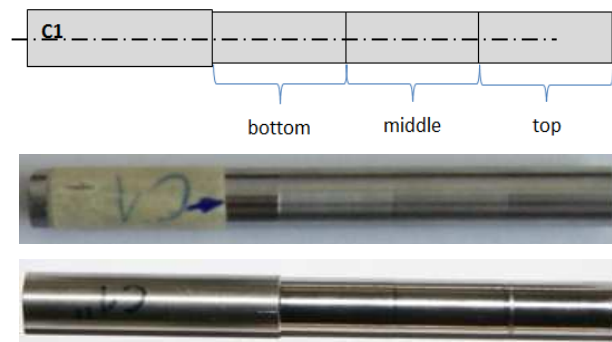


**Figure 5.** Areas of the C1 and C1'' samples subjected to machining.

#### 4. The results of investigation

Figure 6 shows an analysis  $Ssk$  and  $Sku$  surface roughness parameters joined in pairs after turning of the titanium alloy, Ti6Al4V. The same machining parameters have been adopted for the same areas of the samples made by the additive technique and those made by the traditional techniques. When analysing the test results, one can see that there is a correlation between the  $Ssk$  and  $Sku$  roughness parameters. In the areas machined with the least and medium feed values (0.1 – 0.15 mm/rev), the obliqueness values,  $Ssk$ , are positive for both samples. This means that the majority of the material is located near the valleys. The  $Ssk$  parameter is useful in monitoring various kinds of wear conditions on the surface.  $Sku$  indicates the presence of very high peaks / deep valleys on the surface of sample C1 C and C1'' C. For the surfaces of the samples machined with the highest feed values (0.2 mm/rev), the  $Ssk$  parameter values are positive for sample C1 C. In this case, the majority of the material is located near the valleys. In the case of the surface of the C1'' C sample, the values of the  $Ssk$  parameter are negative. Increase of the feed value has resulted in flattening of the vertices on the machined surface. Most of the analysed results show right-hand side asymmetry regardless of the feed. An exception is the surface of sample C1'' C where left-hand side asymmetry can be found.

After the determination of the surface roughness parameters, the technological surface has been shown in a graphic form. This analysis consists in the assessment of the collected 3D surface points

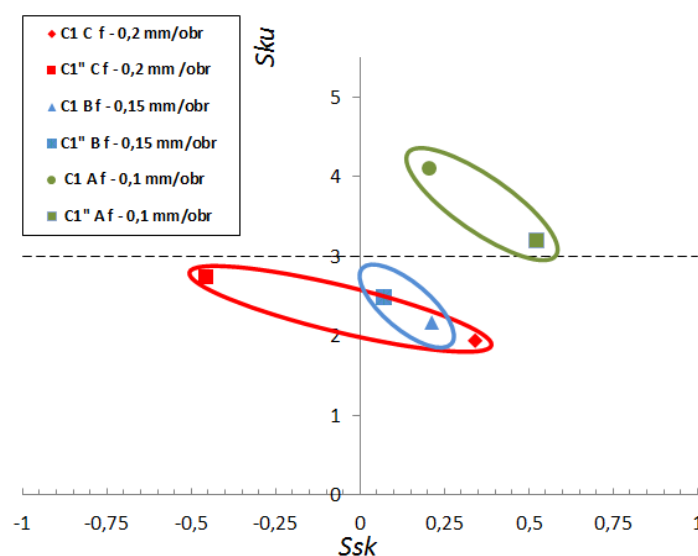


**Figure 6.** Pair of surface roughness parameters: kurtosis ( $Sku$ ) as compared to obliqueness ( $Ssk$ ) after turning as a function of the feed for the cutting speed of  $v_c = 60$  m/min and  $a_p = 0.5$  mm.

and presenting them in the form of contour maps and isometric images. The view of the surface topography has been visually analysed in order to present the turning process characteristics. The analysis has revealed some particular features of the surface influencing the functional properties. Figures 7 and 8 show the surfaces of samples C1 A and C1'' A after turning with the lowest values of the cutting parameters ( $v_c = 60$  m/min,  $f = 0.1$  mm/rev,  $a_p = 0.5$  mm). Crests characteristic of the process of turning have been observed on the surface, resulting from the influence of the feed. In the isometric image (Figures 7b and 8b), one can see single peaks on the surface (marked by red ellipse).

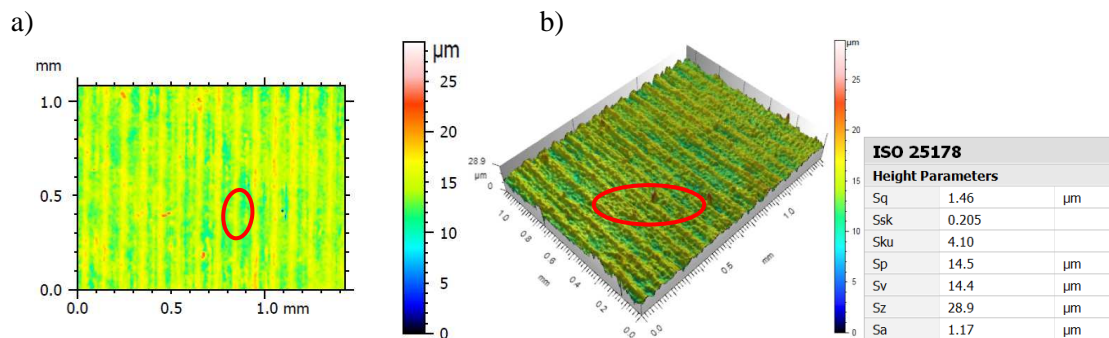


**Figure 7.** Contour map (a) and isometric view (b) of the surface of C1 A sample made of the Ti6Al4V titanium alloy after turning for  $v_c = 60$  m/min,  $f = 0.1$  mm/rev;  $a_p = 0.5$  mm.

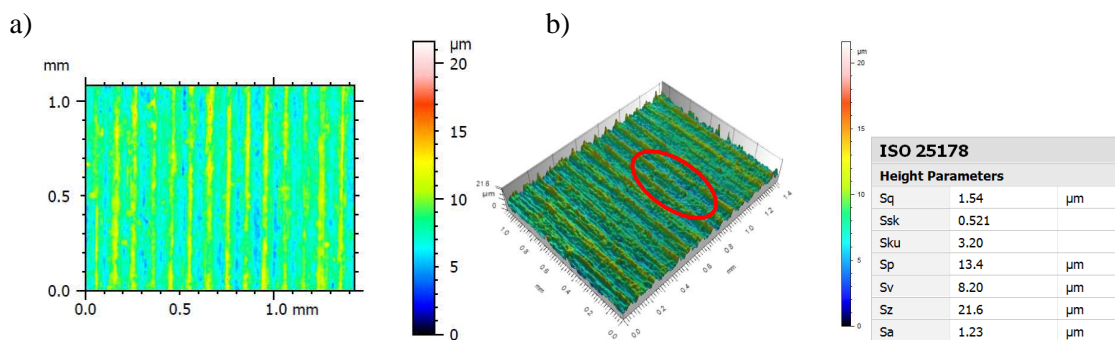


**Figure 8.** Contour map (a) and isometric view (b) of the surface of C1'' A sample made of the Ti6Al4V titanium alloy after turning for  $v_c = 60$  m/min,  $f = 0.1$  mm/rev;  $a_p = 0.5$  mm.

On the surface of sample C1'' A made in the traditional way and shown in Figure 8, one can see periodicity characteristic of the turning operation and one small unevenness. Figures 9 and 10 show the surface of samples C1 B and C1'' B after turning with the cutting parameters ( $v_c = 60$  m/min,  $f = 0.15$  mm/rev,  $a_p = 0.5$  mm).

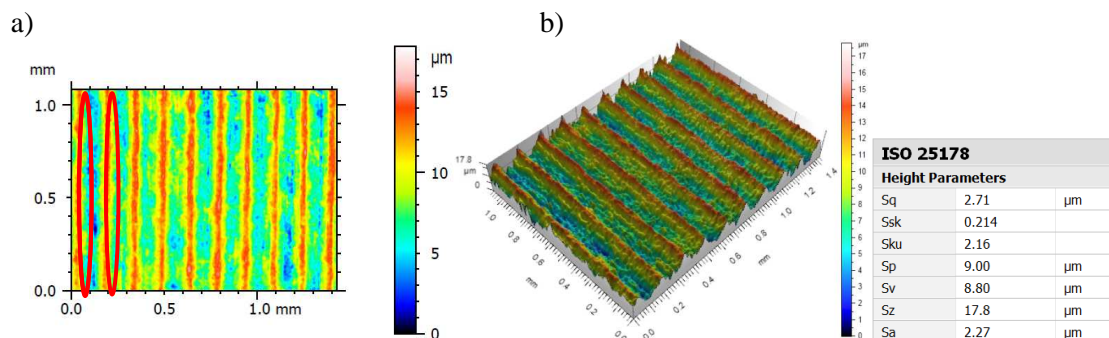


**Figure 9.** Contour map (a) and isometric view (b) of the surface of C1 B sample made of the Ti6Al4V titanium alloy after turning for  $v_c = 60$  m/min,  $f = 0.15$  mm/rev;  $a_p = 0.5$  mm.

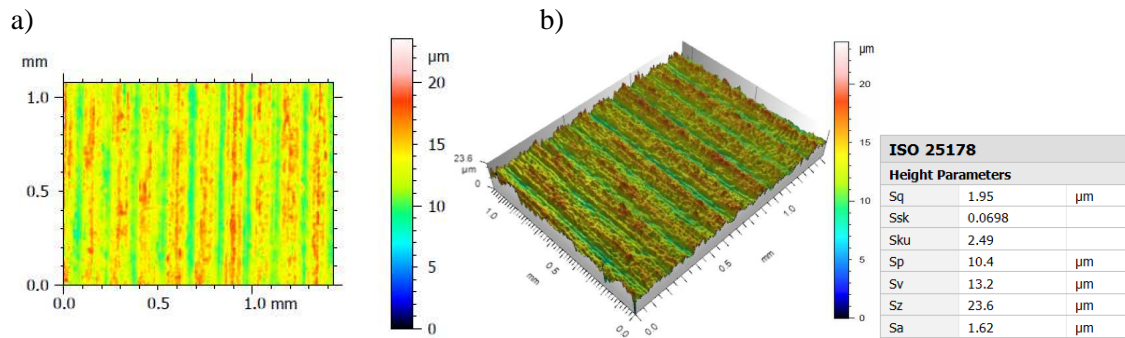


**Figure 10.** Contour map (a) and isometric view (b) of the surface of C1''B sample made of the Ti6Al4V titanium alloy after turning for  $v_c = 60$  m/min,  $f = 0.15$  mm/rev;  $a_p = 0.5$  mm.

The surface C1 C shown in Figure 11 is very uniform. It has even distribution of valleys and crests and characteristic periodicity of the geometrical structure. It can be observed that the width of the crests and valleys is smaller than that for sample C1' C shown in Figure 12. No single peaks or pits occur on the surface.

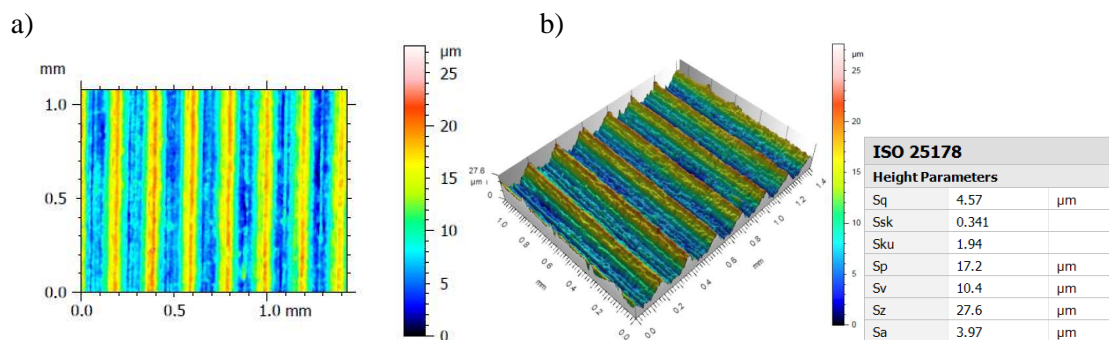


**Figure 11.** Contour map (a) and isometric view (b) of the surface of C1 C sample made of the Ti6Al4V titanium alloy after turning for  $v_c = 60$  m/min,  $f = 0.2$  mm/rev;  $a_p = 0.5$  mm.

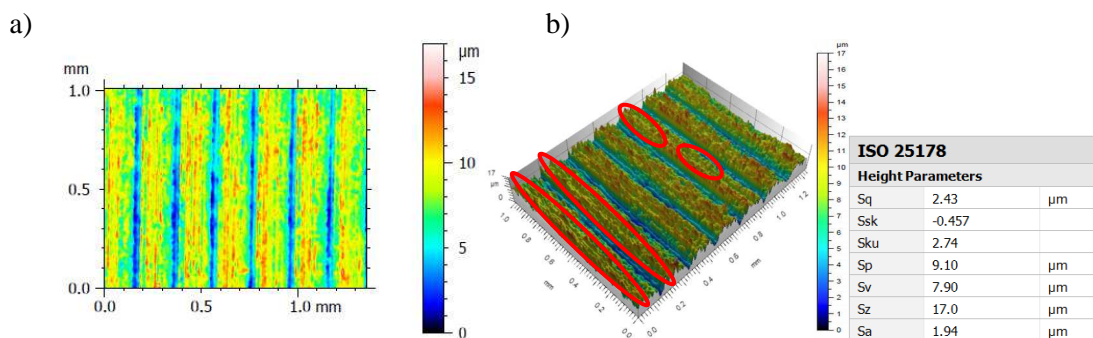


**Figure 12.** Contour map (a) and isometric view (b) of the surface of C1'' C sample made of the Ti6Al4V titanium alloy after turning for  $v_c = 60$  m/min,  $f = 0.1$  mm/rev;  $a_p = 0.5$  mm.

Increase of the feed value up to 0.2 mm/rev, for a surface made by turning, has caused significant changes of the average roughness for sample C1'' C. On the surface shown in Figure 12 b), one can see many irregularities (marked by red ellipses), both valleys and single peaks. In practice, surface topography is influenced by many factors, such as cutting parameters or cutting edge wear. The shape of the surface geometrical structure is a function of the adopted way of machining, its kinematics and technological parameters. The distribution of the characteristic traces of machining on the surface, their regularity or randomness is determined by the degree of the structure isotropy. Isotropy of a

surface geometrical structure means equal surface structure in all directions. It is a perfectly symmetrical structure in relation to all possible symmetry axes. An anisotropic surface is a one which has various topographic features in various directions. Isotropy is expressed as percentage: from 0% (totally anisotropic surface up to 100% (totally isotropic surface). The following conventional division of the isotropy degree is adopted:  $I_s < 20\%$  - anisotropic surface,  $I_s > 80\%$  - isotropic surface,  $20\% < I_s < 80\%$  hybrid structure [12]. The surfaces after machining have more or less privileged direction due to the kinematics of the machining process. The surfaces of samples C1 and C1'' after machining have isotropy in the range of 3.53% to 7.64% - in this case we can speak about an anisotropic surface. Table 1 shows the values of isotropy of the individual samples. The application of various feed values significantly influences increase of isotropy. Isotropy grows with the increase of the feed. Those growths are comparable both for the sample made by the additive technique and the one made by the traditional technique. In the case of sample C1 A, for the feed of 0.1 mm/rev isotropy is 3.53% and increases up to 7.64% for the feed of 0.2 mm/rev. In the case of sample C1'' A, for the feed of 0.1 mm/rev, isotropy is 3.71% and increases up to 6.56% for the feed of 0.2 mm/rev. In order to obtain a more full image, Figure 13 shows the recorded changes of isotropy for various values of machining parameters.

**Table 1.** Machining parameters and isotropy values.

Sample	C1			C1''		
	A	B	C	A	B	C
Area	A	B	C	A	B	C
$v_c$ - m/min	60	60	60	60	60	60
$f$ - mm/ rev	0,1	0,15	0,2	0,1	0,15	0,2
$a_p$ - mm	0,5	0,5	0,5	0,5	0,5	0,5
Isotropy	3,53%	5,79%	7,64%	3,71%	4,95%	6,56%
First Direction	90,0°	90,0°	89,9°	89,9°	89,9°	89,9°
Second Direction	84,6°	37,3°	84,6°	84,6°	84,6°	84,5°
Third Direction	95,4°	66,3°	95,5°	95,4°	66,3°	95,5°

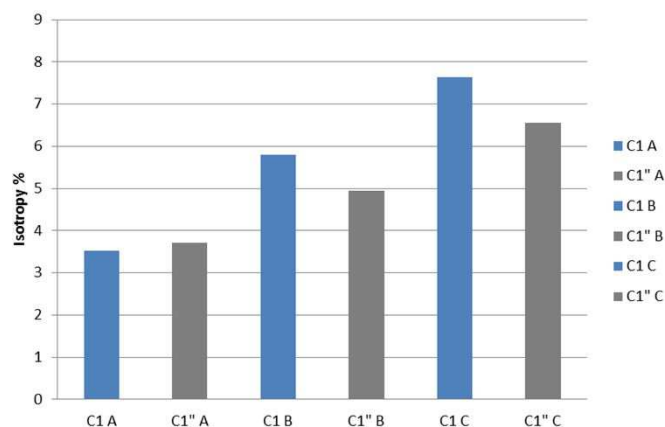


**Figure 13.** Recorded changes of the degrees of isotropy for various values of the machining parameters.

In Figure 14, for example, one can see polar diagrams of the surface isotropy samples C1 A and C1'' A after turning with the smallest values of the feed ( $f = 0.1$  mm/rev). Both the surfaces under examination are characterised anisotropic structure and the isotropy differences between the two surfaces amount to 0.18%. Less feed values result in less disturbances on the surface and the surface is executed more precisely.

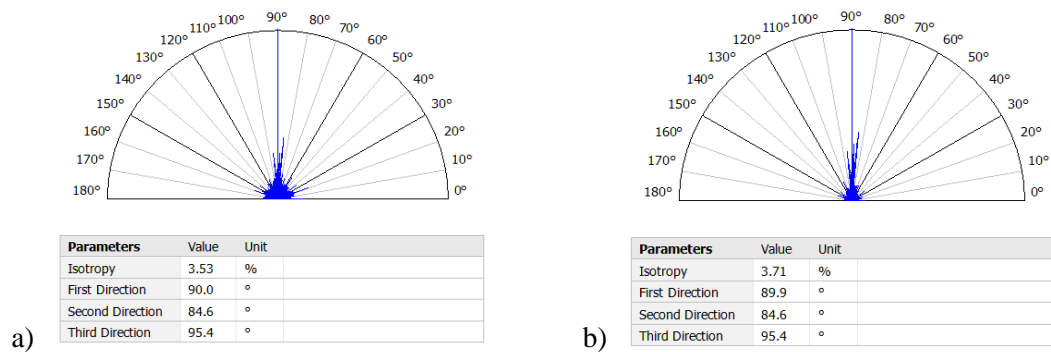


**Figure 14.** Analysis of the sample isotropy: a) C1 A,  $f = 0.1$  mm/rev; b) C1''A,  $f = 0.1$  mm/rev.

Surface isotropy can be an important indication in the process of forming constructional surfaces. Particularly, when improvement of productivity, functionality or part life is concerned in industrial applications. Analysis of the way of surface finishing and forming the surface geometrical structure can improve the general quality of parts influencing the condition of the constructional surfaces in a complex way. Analysing the isotropy results of the surface structure in the process of turning as obtained in the investigation, one can observe an influence of the feed on the surface isotropy. Increase of the feed value reduces the surface anisotropy and, consequently, causes uniform surface structure parameters in all directions. Another topography element under analysis was the Abbott-Firestone curve which describes material distribution in the profile [13], [14]. It is to be considered as a percentage increase of the individual topography points in the structure of the whole surface. From the mathematical point of view, the diagram can be considered as the distribution of probability of the presence of appoint with the height less than that for the read coordinates in the area. On that basis, one can read the properties of the given profile in respect of the utilization functions of the surface geometrical structure [15]. The material contribution curve determines the percentage of the cut material in relation to the covered area. The horizontal axis represents the carrying factor in percentage, the vertical axis is the depth determined in the measurement units [16]. The material contribution curve, in combination with the histogram of the distribution of the function of the ordinates amplitude is a tool for describing the texture of the object under examination. The histogram shows the density of the location of points in the profile under analysis [17]. The material contribution curve gives significant information on the surface condition in respect of its exploitation usability [18]. Figure 15 shows examples of the material contribution curves of the surfaces of sample C1 A and C1'' A after turning for the cutting speed of  $v_c = 50$  m/min,  $f = 0.1$  mm/rev,  $a_p = 0.5$  mm.

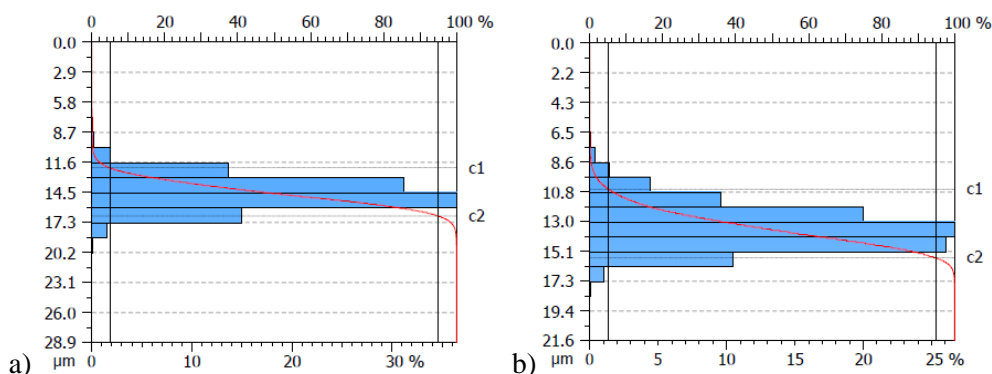


**Figure 15.** Material contribution curve of the surfaces of samples: a) C1 A,  $f = 0.1$  mm/rev; b) C1'' A,  $f = 0.1$  mm/rev.

The surface of a sample made by the additive technique has more concentrated distribution of the density of ordinates than the surface of a sample made by the traditional technology. The most concentrated distribution is that of the surface of sample C1 A – 90% of the material is concentrated within the range of 4.60  $\mu\text{m}$ . The surface of sample C1” A reveals a better exploitation usability – the point of the curve inflexion moves in the degressive direction. In the surface of sample C1 A, over 35 % of the material is concentrated at the height of 15  $\mu\text{m}$ ; in the surface of sample C1” A, over 25% of the material is concentrated at the height of 14  $\mu\text{m}$ .

## 5. Conclusions

Nowadays, 3D topographic surface analysis is more and more popular in industry and it seems that its role in designing and manufacturing will be more and more important in future. 3D measurements of roughness are used for better understanding of the surface nature. All the questions of matching two surfaces concern 3D phenomena, therefore description of them must not be limited to the analysis of the profile. It is particularly important in the case of contact of two matching parts.

On the basis of the executed tests, the following conclusions can be formulated:

- Most of the analysed results, regardless of the feed, indicate right-hand side asymmetry. An exception is the surface of sample C1” C, where left-hand side asymmetry is present.
- Increasing of the feed value up to 0.2 mm/rev has caused significant changes of the average roughness of the surface made by turning in the case of sample C1” C. The surface shows many irregularities, both valleys and single peaks.
- The surfaces of samples C1 and C1” after machining have isotropy in the range of 3.53% to 7.64% - they are, therefore, anisotropic surfaces. Increasing the feed value reduces the anisotropy of the surface resulting in uniform surface structure parameters in all directions.
- The surfaces of samples C1 and C1” which had been subjected to finish machining show degressive-progressive curves of material contribution.

Further investigation should include the assessment of functional parameters, such as: the depth of the core,  $Sk$ , reduced height of the peak,  $Spk$ , reduced depth of the valleys,  $Svk$ , top carrying surface,  $Sr1$ , bottom carrying surface,  $Sr2$ , area of upgrades filled with material,  $Sa1$ , and the area of cavities free from material,  $Sa2$ . A functional analysis of the surface should also be performed based on four volumetric parameters: volume of material peak,  $Vmp$ , volume of material core,  $Vmc$ , volume of the void space core,  $Vvc$ , and the volume of the cavity void space,  $Vvv$ .

## References

- [1] Franco L A and Sinatora A 2015 3D Surface Parameters (ISO 25178-2): Actual Meaning of  $Spk$  and its Relationship to  $Vmp$ , *Precision Engineering* **40** 106-111
- [2] Grobelny P, Furmanski L and Legutko S 2017 *Investigations of Surface Topography of Hot Working Tool Steel Manufactured with the Use of 3D Print*, 13<sup>th</sup> International Conference Modern Technologies in Manufacturing MTeM, Cluj-Napoca, Romania, October 12-13, pp. 137-143
- [3] Ciurana J, Hernandez L and Delgado J 2013 Energy Density Analysis on Single Tracks Formed by Selective Laser Melting with CoCrMo Powder Material, *The International Journal of Advanced Manufacturing Technology* **680**(5-8) 1103-1110
- [4] Nieslony P, Krolczyk G M, Wojciechowski S, Chudy R, Zak K and Maruda R W 2018 Surface Quality and Topographic Inspection of Variable Compliance Part after Precise Turning, *Applied Surface Science* **435** 91-101
- [5] Boyer R R 1996 An Overview on the Use of Titanium in the Aerospace Industry, *Materials Science and Engineering* **213**(1-2) 103-114
- [6] Carl T F Ross 2005 A Conceptual Design of an Underwater Missile Launcher, *Ocean Engineering*, **32**(1) 85-99
- [7] Ross C T F 2006 A Conceptual Design of an Underwater Vehicle, *Ocean Engineering* **33**(16) 2087-2104
- [8] Gorynin I V 1999 Titanium Alloys for Marine Application, *Materials Science and Engineering*

**263**(2) 112-116

- [9] Chunxiang C, BaoMin H, Lichen Z and Shuangjin L 2011 Titanium Alloy Production Technology, Market Prospect and Industry Development, *Materials & Design* **32**(3) 684-1691
- [10] Kosaka Y, Faller K and Fox S P 2004 Newly Developed Titanium Alloy Sheets for the Exhausted Systems of Motorcycles and Automobiles, *JOM* **56**(11) 32-34
- [11] Wierzchoń T, Czarnowska E and Krupa D 2004 *Inżynieria powierzchni w wytwarzaniu biomateriałów tytanowych*, Oficyna Wydawnicza Politechniki Warszawskiej
- [12] Oczóś K 2003 *Struktura geometryczna powierzchni: podstawy klasyfikacji z atlasem charakterystycznych powierzchni kształtowanych*, Oficyna Wydawnicza Politechniki Rzeszowskiej
- [13] Abbott E J and Firestone F A 1933 Specyfing Surface Quality, *Mechanical Engineering* **55** 556-572
- [14] Pawlus P 2006 *Topografia powierzchni: pomiar, analiza, oddziaływanie*, Oficyna Wydawnictwa Politechniki Rzeszowskiej
- [15] Nyc R 2001 Ocena zużycia współpracujących powierzchni elementów maszyn na podstawie krzywych nośności, *Tribologia* **3** 349-355
- [16] Zawada-Tomkiewicz A and Storch B 2016 Analiza struktury geometrycznej powierzchni z wykorzystaniem krzywej udziału materiału, *Mechanik* **11** 1728
- [17] Nadolny K and Kapłonek W 2014 Analysis of Flatness Deviations for Austenitic Stainless Steel Workpieces after Efficient Surface Machining, *Measurement Science Review* **14**(4) 204-212
- [18] Adamczak S 2008 *Pomiary geometryczne powierzchni. Zarysy kształtu, falistość i chropowatość*, Wydawnictwa Naukowo – Techniczne
- [19] Grabon W, Pawlus P, Koszela W and Reizer R 2014 Proposals of Methods of Oil Capacity Calculation, *Tribology International* **75** 117-122